Kinetics and Mechanism of Nitric Oxide Disproportionation upon Reaction with Ruthenium(II) Porphyrin Carbonyls: Evidence for Dinitrosyl Intermediates[1]

Ivan M. Lorković and Peter C. Ford*

Department of Chemistry, University of California, Santa Barbara, California 93106

Received September 18, 1998

The kinetics of the reaction of nitric oxide with the ruthenium porphyrin carbonyl complexes Ru(P)(CO) (P = octaethylporphyrin (OEP) or tetra-*m*-tolylporphine (TmTP)) to give the respective nitrosyl nitrito complexes Ru(P)(NO)(ONO) plus N_2O were studied by stopped flow spectrophotometric techniques. Temporal spectral changes proceed in two stages via formation of an easily discernible intermediate **X**. The rates of both stages are first order in ruthenium concentration. In the NO concentration range 40−400 μM, the rate law of the first stage is first order in [NO], but the slower second stage displays a rate law second order in [NO]. In the presence of some added CO, it is possible to demonstrate that the equilibrium between Ru(P)(CO) and **X** has a second-order dependence on [NO]. As a consequence, it is concluded that **X** is the dinitrosyl complex $Ru(P)(NO)_2$. No other intermediates develop sufficient concentrations to be observable by the stopped flow method. The kinetics behavior of this system is interpreted in terms of a rate-limiting step in the first stage involving CO dissociation from a reactive intermediate Ru(P)(CO)(NO) formed in very low concentrations by the reversible addition of NO to Ru(P)(CO). Several hypothetical mechanisms for the second stage are considered, and it is concluded that the evidence is most consistent with a pathway where the Ru center serves as a template to assemble an oligomer of NO which decomposes to nitrous oxide plus coordinated nitrite.

Introduction

Nitric oxide is now known to have key roles in human cardiovascular and nervous systems and in immune response to pathogen invasion.[2] These discoveries have stimulated much interest in compounds that can deliver NO to biological targets upon demand either by thermal reactions or by photochemical excitation.[3] In the course of probing photochemical precursors,[4] studies in this laboratory turned to the synthesis of nitrosyl ruthenium porphyrin complexes by reaction of NO with the carbonyl analogues Ru(P)(CO) (**1**) (**1a**, P = TPP (tetraphenylporphyrin); **1b**, P = OEP (octaethylporphyrin)).[5] Notably, this reaction was accompanied by disproportionation of NO. In each case, the principal ruthenium product isolated was the nitrosyl nitrito complex Ru(P)(NO)(ONO) (**2b** and **2c** for the respective porphyrins), and N_2O was also formed in the approximately correct stoichiometry (eq 1).[5] (The respective nitrosyl hydroxo complex Ru(P)(NO)(OH) (**3**) was a minor product under synthetic conditions.) Several other recent reports have also described syntheses of **2** and related nitrosyl ruthenium porphyrin complexes.[6]

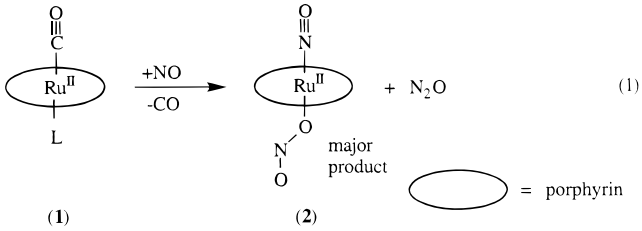

(1)

Equation 1 is but one example of metal-activated NO disproportionations that are especially prevalent in the literature regarding the synthesis of nitrosylmetalloporphyrin complexes[7] and have been reported for other metal complexes.[8] Thus, to gain better insight into such metal-mediated redox processes of NO, we initiated the present investigation into the kinetics and time-resolved spectra of intermediates along the reaction coordinate outlined by eq 1. The ruthenium substrates studied

(1) Reported at the 214th National Meeting of the American Chemical Society, Las Vegas, Nevada, September 1997. Abstract: *Inorg. 420.*

(2) (a) Palmer, R. M. J.; Ferrige, A. G.; Moncada, S. *Nature* **1987**, *327*, 524−526. (b) Ignarro, L. J.; Buga, G. M., Wood, K. S., Byrns, R. E.; Chaudhuri, G. *Proc. Natl. Acad. Sci., USA.* **1987**, *84*, 9265−9269. (c) Hibbs, J. B., Jr.; Taintor, R. R.; Vavrin, Z. *Science* **1987**, *235*, 473−476. (d) Furchgott, R. F.; Vanhoute, P. M. *FASEB J.* **1989**, *3*, 2007−2018. (e) Moncada, S.; Palmer, R. M. J.; Higgs, E. A. *Pharmacol. Rev.* **1991**, *43*, 109−142. (f) Feldman, P. L.; Griffith, O. W.; Stuehr, D. J. *Chem. Eng. News* **1993**, *71*, 10, 26−38. (g) Wink, D. A.; Hanbauer, I.; Grisham, M. B.; Laval, F.; Nims, R. W.; Laval, J.; Cook, J.; Pacelli, R.; Liebmann, J.; Krishna, M.; Ford, P. C.; Mitchell, J. B. *Curr. Top. Cell. Regul.* **1996**, *34*, 159−187. (h) Feelish, M., Stamler, J. S., Eds. *Methods in Nitric Oxide Research*; John Wiley and Sons: Chichester, England, 1996, and references therein.

(3) Feelish, M.; Stamler, J. S. Chapter 7 in ref 2h, pp 71−113.

(4) (a) Hoshino, M.; Ozawa, K.; Seki, H.; Ford, P. C. *J. Am. Chem. Soc.* **1993**, *115*, 9568−9575. (b) Bourassa, J.; DeGraff, W.; Kudo, S.; Wink, D. A.; Mitchell, J. B.; Ford, P. C. *J. Am. Chem. Soc.* **1997**, *119*, 2853−2860.

(5) (a) Miranda, K. M.; Bu, X.; Lorkovic, I.; Ford, P. *Inorg. Chem.* **1997**, *36*, 4838−4848. (b) Miranda, K. M., Ph.D. Dissertation, UC Santa Barbara, 1996.

(6) (a) Kadish, K. M.; Adamian, V. A.; Caemelbecke, E. V.; Tan, Z.; Tagliatesta, P.; Bianco, P.; Boschi, T.; Yi, G.-B.; Khan, M. A.; Richter-Addo, G. B. *Inorg. Chem.* **1996**, *35*, 1343−1348. (b) Bohle, D. S.; Goodson, P. A.; Smith, B. D. *Polyhedron* **1996**, *15*, 3147−3150. (c) Yi, G.-B.; Khan, M. A.; Richter-Addo, G. B. *J. Chem. Soc., Chem. Commun.* **1996**, 2045−2046. (d) Yi, G.-B.; Khan, M. A.; Richter-Addo, G. B. *Inorg. Chem.* **1996**, *35*, 3453−3454. (e) Hodge, S. J.: Wang, L.-S.; Khan, M. A., Young, V. G.; Richter-Addo, G. B. *J. Chem. Soc., Chem. Commun.* **1996**, 2283−2284. (f) Bohle, D. S., Hung, C.-H.; Smith, B. D. *Inorg. Chem.* **1998**, *37*, 5798−5706.

(7) (a) Yoshimura, T. *Inorg. Chim. Acta* **1984**, *83* 17−21. (b) Nasri, H.; Ellison, M. K.; Chen, S. Huynh, B. H.; Scheidt, W. R. *J. Am. Chem. Soc.* **1997**, *119*, 6274−6283.

10.1021/ic981121r CCC: $18.00
Published on Web 03/19/1999

were **1b** and Ru(TmTP)(CO) (**1c**, TmTP = tetra-*m*-tolylporphine), which is a more soluble analogue of **1a**. During the course of these studies, spectral evidence was also obtained indicating the formation of the dinitrosyl analogues $Ru(P)(NO)_2$ (**4b** and **4c**) under specific solution conditions.

Experimental Section

Materials. Tetra-*m*-tolylporphine (H_2TmTP) and Ru(OEP)(CO) were purchased from Midcentury Chemicals Inc. (Posen, IL). Ru(OEP)(CO) was further purified by chromatography on silica/CH_2Cl_2 and found pure by ^{1}H NMR. The preparation for **2b** has been previously described and can be accomplished by the procedure for **2c** described below. All other reagents were obtained from commercial sources and purified according to established procedures. Toluene was distilled from a purple solution of benzophenone over sodium and stored under either vacuum or Ar. NO (99.0% purity; Matheson) was purified of higher nitrogen oxides by passage through a stainless steel column, containing Ascarite II (NaOH on a silicate carrier; Thomas Scientific).

The carbonyl complex Ru(TmTP)(CO) (**1c**) was prepared by refluxing a toluene solution (50 mL/g of combined reagents) containing ~2.5 equiv of $Ru_3(CO)_{12}$ with 1 equiv of free base for 18 h reflux under static Ar. After toluene removal in vacuo, the residue was purified by chromatography on silica, starting with 50/50 CH_2Cl_2/pentane, which elutes any remaining $Ru_3(CO)_{12}$ and free base H_2TmTP sequentially and separately. After the CH_2Cl_2/pentane ratio was increased, the product eluted as a bright orange-red band and the solid was recovered by evaporation of the solvent (50−75% yield based on H_2TmTP). ^{1}H NMR, $CDCl_3$, δ vs TMS: 8.71 (8H, s), 7.99 (8H, m), 7.59 (8H, m) 2.62 (12H, s). IR, CH_2Cl_2: $\nu_{CO} = 1941$ cm^{-1}). FABMS: NBA matrix, $+m/z$ (relative intensity, assignment) Calculated most abundant parent mass (M) for $RuC_{49}H_{36}N_4O$: 798. Observed: 799 (0.15, M + H$^+$), 798 (0.70, M$^+$), 770 (1.00, M$^+$ − CO).

The nitrosyl nitrito species Ru(TmTP)(NO)(ONO) (**2c**) was prepared as follows. A CH_2Cl_2 solution of Ru(TmTP)(CO) was added to a flask of appropriate volume sealed with an airtight Teflon valve. After degassing the solution, NO (at least 6 equiv) was condensed into the flask (at 77 K) from a gas transfer vacuum line, but care was taken so that the total pressure after thawing including 400 Torr CH_2Cl_2 did not exceed 1100 Torr at room temperature. The contents of the flask were stirred at room temperature (1 h), and then the volatile constituents were removed by condensation into a coldfinger at 77 K. The solid residue was dissolved in a CH_2Cl_2/pentane mixture and chromatographed on silica using the same conditions as for Ru(TmTP)(CO). The olive/wine product band was identical in appearance to Ru(TPP)(NO)(ONO).[5] In $CDCl_3$ the ^{1}H NMR spectrum of **3** was of high symmetry, showing only one sharp tolyl methyl peak, consistent with free rotation of the *m*-tolyl group. However, in room-temperature C_6D_6, the spectrum was more complicated. The pyrrole β proton peak (9.01 ppm) exhibited a number of shoulders, while the *m*-tolyl methyl protons appeared as two equal singlets at 2.26 and 2.34 ppm, representing cis and trans orientations of the methyl groups with respect to the axial ligands. At 60 °C the β-pyrrole resonances collapsed into a single symmetric peak, while the two methyl peaks, being further separated, remained distinct. This behavior suggests atropisomer interconversion (by tolyl rotation) with lifetimes on the order of seconds at room temperature. The barrier to rotation of the tolyl moiety appears to be higher in C_6D_6 than in $CDCl_3$, making atropisomers observable in C_6D_6 at ambient temperature. ^{1}H NMR, $CDCl_3$, δ vs TMS: 9.01 (8H, s), 8.10 (8H, m), 7.65 (8H, m), 2.65 (12H, s). IR, cyclohexane, cm^{-1} (ϵ, M^{-1} cm^{-1}): 1842 (3300, ν_{NO}), 1526 (750, $\nu_{(as)ONO}$). IR, toluene, cm^{-1} (ϵ, M^{-1} cm^{-1}): 1845 (1300, ν_{NO}). UV−vis (toluene), nm (ϵ, M^{-1} cm^{-1}): 411 (2.0×10^5), 561 (10.2×10^4), 606 (s). FABMS: NBA matrix, $+m/z$ (relative intensity, assignment) Calculated most abundant parent mass (M) for $RuC_{48}H_{36}N_6O_3$: 846. Observed: 817 (0.05, M − NO + H$^+$), 800 (1.00, M − ONO$^-$), 786 (0.24, M$^+$ − 2NO), 770 (0.34, M − NO − ONO$^-$).

After elution of **2c** from the above column, a second compound eluted as a concise deep red band by addition of CH_2Cl_2 containing 3% MeOH. This was identified as the nitrosyl hydroxo complex Ru(TmTP)(NO)(OH) (**3c**) by its chromatographic and spectroscopic similarity to the well characterized analogue Ru(TPP)(NO)(OH).[4] ^{1}H NMR, $CDCl_3$, δ vs TMS: 9.03 (8H, s), 8.10 (4H, m), 8.02 (4H, m) 7.67 (8H, m), 2.67 (6H, s) 2.63 (6H, s). IR, toluene, cm^{-1} (ϵ, M^{-1} cm^{-1}): 1812 (1100, ν_{NO}). UV−Vis, toluene, nm (ϵ, M^{-1} cm^{-1}): 414 (1.0×10^5), 556 (1.8×10^4), 594 (6100). FABMS; NBA matrix, $+m/z$ (rel int., assignment) Calculated most abundant parent mass (M): 817. Observed: 817 (0.10, M$^+$), 800 (1.00, M − OH$^-$), 786 (0.24, M$^+$ − HNO), 770 (0.34, M − NO − OH$^-$).

Instrumentation. Optical spectra in solution were recorded on a HP-8452a diode array spectrophotometer with ~2 nm resolution. Infrared spectra were recorded with a Bio-Rad FTS-60 or Mattson Research FTIR spectrophotometers. NMR spectra were obtained on Varian 200, 400, and 500 MHz spectrometers in $CDCl_3$ ($CHCl_3$ at 7.260 ppm). FAB mass spectra (xenon atom bombardment of a 3-nitrobenzyl alcohol matrix) were obtained on a VG 70E double-focusing mass spectrometer.

Kinetics Procedures and Instrumentation. Kinetics experiments were performed on an Applied Photophysics SX-17MV stopped flow spectrophotometer equipped with both a double monochromator/PMT single wavelength detection system (<1 nm resolution) and a rapid-scan diode array detector (~7 nm resolution). For general reaction features, including isosbestic point determination and stacked plot generation on a rapid time scale, the diode array system was appropriate, although distortions of sharp absorptions were noticeable. Therefore, all quantitative measurements (rate, extent of reaction, reaction order, etc.) were obtained using the higher resolution single-wavelength method. For working with highly air-sensitive solutions, several custom modifications were introduced to the stopped flow instrumentation. For example, the thermostat fluid circulating from a constant-temperature bath throughout the rapid mixing apparatus was purged with N_2. In addition, the tubing connecting the syringe containing NO solutions to the mixing cell was changed to stainless steel (Upchurch precut), which was connected to the glass cell with "super flangeless" fittings (Upchurch), taking care that metal did not touch glass. PEEK tubing was used to connect the syringe containing the metal porphyrin solution to the mixing cell.

All manipulation of porphyrin solutions was performed so as to minimize exposure to light. Although no special precautions must be taken besides standard Schlenk techniques in the syntheses, the kinetics of the reaction of **1c** with NO are profoundly influenced by the presence of trace oxygen and water (vide infra). For this reason, extra precautions were taken in preparing and handling solutions. To prepare and transfer toluene solutions of known [NO] and [Ru] to the drive syringes, specially modified tonometers were fabricated (Figure S-1 in Supporting Information). These used Chemglass airless, greaseless valves at all points of entry in addition to a 7 mm O-ring adapter to allow connection to an all-glass/Teflon vacuum/NO line. For convenience, the toluene solutions were transferred to the tonometers in an inert atmosphere box. Nitric oxide solutions were prepared by vacuum transfer of purified NO at known pressures, temperatures, and volumes into tonometers of known volume (~180 mL) containing previously degassed toluene frozen in a LN_2 coldfinger. The NO/toluene solutions were warmed to room temperature, and then Ar was admitted to give a total pressure of 820 Torr. After detachment from the vacuum line, the tonometers were vigorously shaken for vapor−liquid equilibration. The NO concentrations were calculated for these solutions using the ideal gas law and the appropriate Ostwald coefficients for NO in toluene.[9] Prior to loading solutions into the stopped flow instrument, the drive syringes, which employ Teflon plungers and valves, were evacuated (to <10 μmHg for at least 6 h). The loaded tonometer was then attached to the drive syringe loading port via the luer tip, and the volume between the

(8) (a) Gwost, D.; Caulton, K. G. *Inorg. Chem.* **1974**, *13*, 414−417. (b) Bottomley, F. In *Reactions of Coordinated Ligands*; Braterman, P. S., Ed.; Plenum Press: New York, 1982; Vol. 2, pp 115−222. (c) McCleverty, J. *Chem Rev.* **1979**, *79*, 53. (d) Ruggiero, C. E.; Carrier, S. M.; Tolman, W. B. *Angew. Chem., Int. Ed. Engl.* **1994**, *33*, 895−897.

(9) Oxides of Nitrogen. *IUAPC Solubility Data Series*, Vol. 8, Young, C. L, Ed.; Pergamon Press: Oxford, 1983.

Table 1. Optical Spectra of Ruthenium Porphyrin Complexes in Ambient Temperature Toluene

compound	λ_{max}, nm (log ϵ)			
		Soret band	Q(1,0)	Q(0,0)
Ru(OEP)CO (**1b**)	376 (4.86)	396 (5.15)	514 (4.15)	546 (4.70)
Ru(OEP)(NO)(ONO) (**2b**)	352^{sh} (4.50)	396 (5.08)	544^{sh} (3.88)	574 (3.92)
Ru(OEP)$(NO)_2$ (**X_b**)	350^{sh} (4.54)	395 (4.95)	532(4.03)	560 (4.09)
Ru(TmTP)CO (**1c**)		412 (5.32)	528 (4.29)	562^{sh} (3.41)
Ru(TmTP)(NO)(ONO) (**2c**)		412 (5.26)	564 (3.95)	606^{sh} (3.60)
Ru(TmTP)(NO)(OH) (**3c**)		414 (5.00)	556 (4.26)	594 (3.79)
Ru(TmTP)$(NO)_2$ (**X_c**)		412 (5.03)	546 (4.10)	585^{sh} (3.61)

tonometer and the drive syringe was evacuated for at least 5 min before transferring solutions to the drive syringes. The drive syringes were flushed and reloaded three times before rate measurements or time-resolved spectra were recorded.

Results and Discussion

Ru(P)(CO) in Toluene. The UV−visible spectra of the carbonyl starting materials **1b** and **1c** in dry toluene are summarized in Table 1 with the spectra of other species of interest to the present study. Solutions of Ru(P)(CO) prepared with a freshly opened bottle of commercial (wet) toluene displayed spectra that have measurable differences from those prepared in rigorously dried toluene. In studies to be reported elsewhere,[10] it was demonstrated that these spectral changes can be attributed to coordination of H_2O to the sixth site on the ruthenium (e.g., eq 2, L = H_2O). Similar spectral changes were noted on adding other donor ligands to solutions of **1b** or **1c**.[10] Attempts to measure the kinetics of this reaction for various L using the stopped flow spectrometer were unsuccessful since the reaction of Ru(P)(CO) with L was too fast. However, from these experiments, a lower limit for the second-order rate constant to form Ru(P)(CO)L could be conservatively estimated as $k_L > 10^5$ M^{-1} s^{-1}.[10]

$$\text{Ru(P)(CO)} + \text{L} \overset{k_L}{\rightleftharpoons} \text{Ru(P)(CO)L} \qquad (2)$$

Reaction of NO with Ru(P)(CO). The reaction of Ru(P)(CO) (**1**) with NO eventually leads to the formation of the nitrosyl nitrito complexes **2b** and **2c**. Notably, the Soret bands are little changed from those of the respective carbonyl analogues **1b** and **1c**; however, the Q band absorptions are broader and occur at longer wavelengths (Table 1). Figure 1 documents temporal optical spectral changes after mixing a solution of Ru(TmTP)(CO) with excess NO in dry toluene recorded with the diode array detector of the stopped flow spectrophotometer. On the time scale of a few milliseconds, **1c** cleanly (with isosbestic points) gives way to an intermediate **X_c** for which the Q band position and width lie between those of **1c** and the final product **2c**. The Soret band does not change position but does show an intensity decrease at its λ_{max} and broadens significantly. On the longer time scale of a few seconds, the spectrum of **X_c** cleanly changes to a final spectrum nearly identical to that of a chromatographically purified sample of **2c** (eq 3). There were no further spectral changes. The temporal spectra during the course of the reaction of Ru(OEP)(CO) with NO to give first **X_b** then **2b** were analogous. Since the sequential reactions have very different time scales, it was possible to obtain semiquantitative spectra of **X_b** and **X_c** from the diode array detector by reaction of **1b** and **1c**, respectively, with excess NO in dry toluene, and these spectra are also summarized in Table 1.

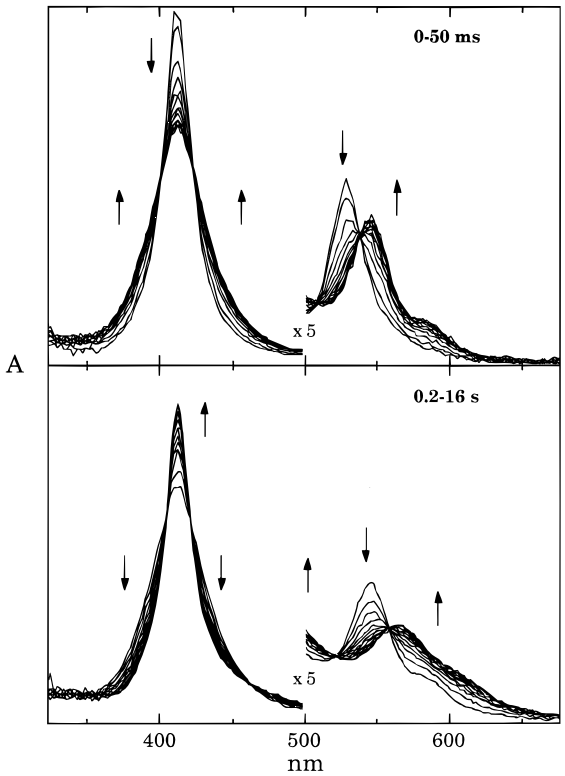

Figure 1. Temporal spectral changes immediately upon mixing toluene solutions of **1c** and NO (initial concentrations after mixing are 20 μM and 1.5 mM, respectively, at 25 °C). Upper: 0−50 ms after mixing. Lower: 0.2−16 s after mixing.

$$\text{Ru(P)(CO)} + \text{xs NO} \xrightarrow{k_{obs}(1)} \mathbf{X} \xrightarrow{k_{obs}(2)} \text{Ru(P)(NO)(ONO)} + \text{N}_2\text{O} + \text{CO} \qquad (3)$$

Kinetics Studies. As noted above, single-wavelength detection using the PMT detector gave superior data for kinetic measurements. This is illustrated by Figure 2, which documents the temporal spectral changes at 412 nm (where maximum spectral changes are observed) upon mixing dry toluene solutions of **1c** and NO to give the respective initial concentrations ~2×10^{-5} and 3.0×10^{-3} M at 25 °C. Both the rapid decrease in absorbance at the Soret band maximum and the subsequent, slower increase can be fit to first-order equations (fits shown as solid lines) indicating that each is first order in [Ru], the limiting reactant. The same general behavior was seen for reaction of Ru(OEP)(CO) with NO.

For both substrates, plots of $k_{obs}(1)$ vs [NO] (with [NO] ranging from 40 to 400 μM and Ru concentrations adjusted to maintain a [Ru]/[NO] ratio of >10) proved to be linear (Figure 3). This indicates that the first step is also first order in [NO]

(10) Lorkovic, I.; Works, C.; Andreasen, L.; Ford, P. C. Manuscript in preparation.

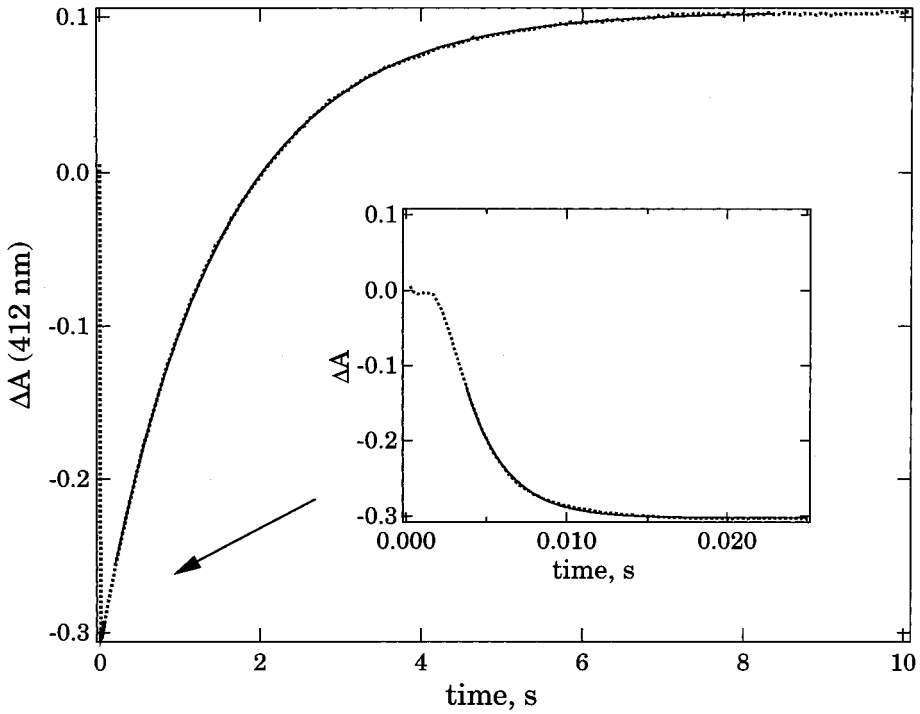

Figure 2. Temporal absorbance changes at 412 nm upon mixing toluene solutions of **1c** and NO (initial concentrations after mixing are 20 μM and 3.0 mM, respectively, at 25 °C). The inset shows the rapid initial decrease in absorbance owing to the formation of $\mathbf{X_c}$, and the larger figure shows the slower recovery of absorbance as **2c** is formed. The solid lines represent fits of experimental data to first-order kinetics models for each of the steps.

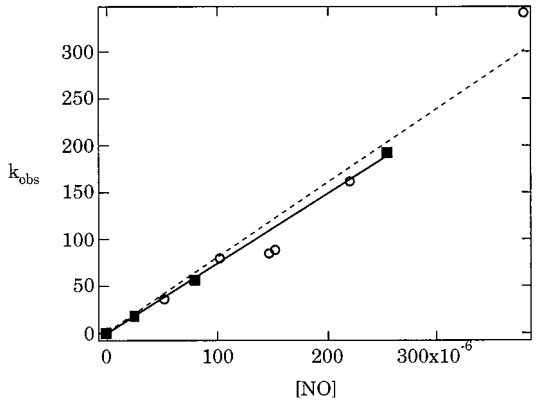

Figure 3. Plots of $k_{obs}(1)$ vs [NO] for the reaction of **1b** (circles) and of **1c** (squares) with NO in 25 °C toluene.

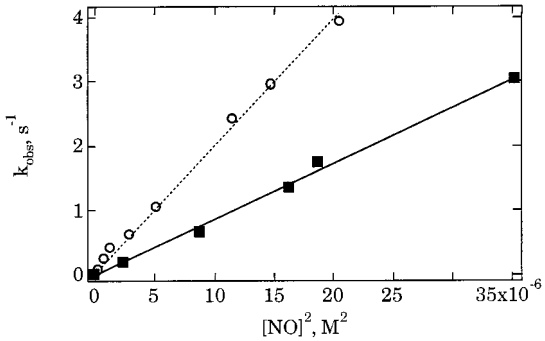

Figure 4. Plot of $k_{obs}(2)$ vs $[NO]^2$ for the reaction of **1b** (circles) and of **1c** (squares) with NO in 25 °C toluene.

Table 2. Kinetic and Equilibrium Data for Ru(P) with CO and NO in 25 °C Toluene

	P = OEP	P = TmTP
k_1, $M^{-1}\,s^{-1}$	$(7.9 \pm 1.5) \times 10^5$	$(7.5 \pm 0.8) \times 10^5$
k_2, $M^{-2}\,s^{-1}$	$(1.9 \pm 0.2) \times 10^5$	$(8.6 \pm 1.0) \times 10^4$
K_{NO}, M^{-1}	$(2.0 \pm 0.4) \times 10^5$	$(6.3 \pm 1.5) \times 10^4$
K_{CO}, M^{-1} [a]	$(1.11 \pm 0.15) \times 10^4$ [a]	$(3.9 \pm 0.3) \times 10^3$ [a]

[a] Data from ref 10.

under these conditions, i.e., $k_{obs}(1) = k_1[NO]$. The resulting second-order rate constants k_1 determined from the slopes of the plots have the values $(7.9 \pm 1.5) \times 10^5$ M^{-1} s^{-1} for P = OEP and $(7.5 \pm 1.0) \times 10^5$ M^{-1} s^{-1} for P = TmTP in 25 °C toluene (Table 2).

At the NO concentrations (0.5−6 mM) convenient for the kinetics studies, the second stage in the stepwise transformation was slower than the first and easily separated in terms of viewing its dynamics. Plots of $k_{obs}(2)$ vs [NO] were nonlinear for both substrates, but plots of $k_{obs}(2)$ vs $[NO]^2$ were linear with intercepts at the origins (e.g., Figure 4). Thus, the rate of the second step appears to be second order in [NO]; that is, $k_{obs}(2) = k_2[NO]^2$ under these conditions. The values of the termolecular rate constants k_2 determined in this manner are $(1.9 \pm 0.2) \times 10^5$ and $(8.6 \pm 1.0) \times 10^4$ M^{-2} s^{-1} for P = OEP and TmTP, respectively (Table 2).[11]

When the same reactions were probed in toluene solutions which had not been rigorously dried, or to which a small concentration of a donor ligand L such as methanol, water, or CO had been added, the $k_{obs}(1)$ values were smaller. In contrast, $k_{obs}(2)$ values for the second step were little affected; thus, under such circumstances, the separation of time scales of the first

(11) Although not seen in Figure 2, it is noteworthy that at low [NO] the spectral change for the slow step becomes bimodal. Also, the rate constant observed, if fit to a single exponential, is much higher than would be expected if the reaction remained second order in [NO]. If exceeding care is taken to exclude even traces of O_2, the onset of bimodal decay occurs at lower [NO]. At higher [NO], the second-order pathway dominates and the competing pathway is not seen. We speculate that the competing pathway is the facile reaction of **X** with N_2O_3 or NO_2 formed by NO autoxidation and present at substoichiometric concentrations.

and second reactions was blurred. These results were concluded to be the result of competition between L and nitric oxide for the sixth coordination site on **1** (see below).

What is X? Since the rate of the second step is dependent on $[NO]^2$, lowering concentrations to near stoichiometric levels slows that reaction much more than the first step. Under such conditions, the absorbance changes and isosbestic points for reactions of both **1b** and **1c** with NO are consistent with formation of the respective intermediates $\mathbf{X_b}$ and $\mathbf{X_c}$, but the magnitudes of the absorbance changes are clearly dependent on P_{NO}. These results serve as evidence for establishing an equilibrium between Ru(P)(CO) and **X** prior to subsequent reaction under these conditions.

$$\underset{\textbf{1b (or 1c)}}{\text{Ru(P)(CO)} + x\text{NO}} \overset{K_{NO}}{\rightleftharpoons} \underset{\mathbf{X_b}\ (\text{or } \mathbf{X_c})}{\text{Ru(P)(NO)}_x} + \text{CO} \qquad (4)$$

Whether **X** is a mononitrosyl or a dinitrosyl complex (i.e., whether x is 1 or 2) may thus be evaluated from the [NO] dependence of this equilibrium, determined spectrally at a single value of [CO]. However, under excess CO, there is the additional complication of equilibrium formation of the dicarbonyl Ru(P)$(CO)_2$ (eq 6), and the effects of this on the overall concentrations of various ruthenium species must be taken into account. Values of K_{CO} in 25 °C toluene have been determined for **1b** and **1c** to be $(1.11 \pm 0.15) \times 10^4$ and $(3.9 \pm 0.3) \times 10^3$ M^{-1}, respectively, from changes in the optical spectra of these complexes in the presence of known concentrations of CO.[10]

$$\text{Ru(P)(CO)} + \text{CO} \overset{K_{CO}}{\rightleftharpoons} \text{Ru(P)(CO)}_2 \qquad (5)$$

To measure K_{NO} accurately, [CO] must be sufficient to be treated as a constant but low enough to avoid suppressing the reactivity to the extent that equilibrium formation of **X** is not reached before significant onset of the second process. These conditions were met at the [CO] values (0.8−2.5 mM) investigated. Elaborating upon the derivation described by Hoshino,[4a] one can obtain the following relationship between the absorbance change ΔA at a certain wavelength during the first step and the concentration of NO added to a solution of **1** (corrected for dilution):

$$\Delta A^{-1} = \Delta A_{tot}{}^{-1}(1 + f_{CO}K_{NO}{}^{-1}[NO]^{-x}) \qquad (6)$$

In this expression, ΔA_{tot} is the absorbance change for complete conversion from the equilibrium mixture of Ru(P)(CO) and Ru(P)$(CO)_2$ to the intermediate **X**, and $f_{CO} = [CO](1 + K_{CO}[CO])$. Thus, for the appropriate x (1 or 2), a plot of ΔA^{-1} versus $[NO]^{-x}$ should be linear, from which K_{NO} can be derived according to

$$K_{NO} = (\text{intercept/slope})f_{CO} \qquad (7)$$

In this context, plots were made of ΔA^{-1} versus both $[NO]^{-1}$ and $[NO]^{-2}$. Such plots for both complexes (Figure 5) gave good linear fits for $x = 2$ and gave reasonable values for intercepts, which for such plots represent $(\Delta A_{tot})^{-1}$. For the experiments described here, this should be between 2 and 10.) In contrast, plots for $x = 1$ were curved upward and gave very small or negative, hence unreasonable, intercepts. Thus, the first stage in the reaction of NO with **1** is concluded to be the reversible formation of the dinitrosyl complex Ru(P)$(NO)_2$ (eq 8) in each case. On the basis of this conclusion, the K_{NO} values of $(2.0 \pm 0.4) \times 10^5$ M^{-1} for **1b** and $(6.3 \pm 1.5) \times 10^4$ M^{-1} for **1c** (Table 2) were determined.

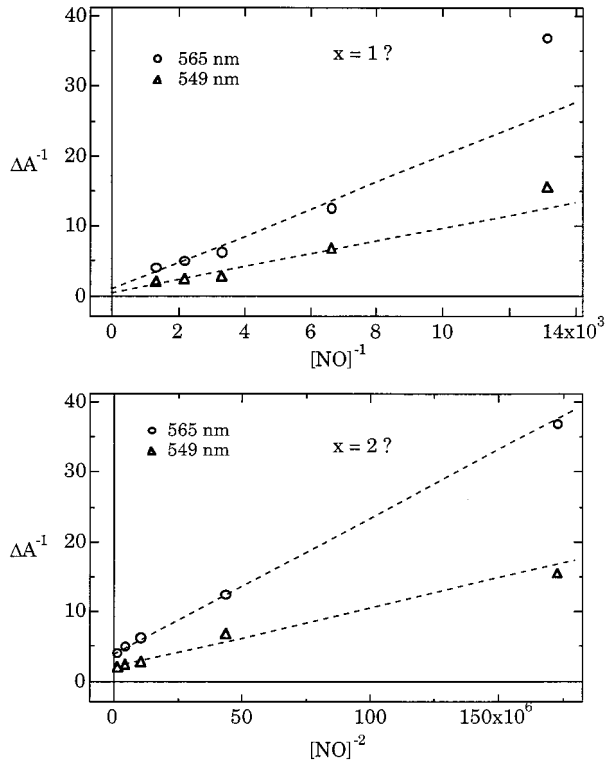

Figure 5. Plots of ΔA^{-1} vs $[NO]^{-1}$ and vs $[NO]^{-2}$ for overall absorbance change for the formation of the intermediate $\mathbf{X_b}$ (eq 1) from **1b**. [CO] = 0.83 mM. The linear fits of ΔA^{-1} vs $[NO]^{-x}$ ($x = 1, 2$) are weighted by ΔA since relative error increases with ΔA^{-1}. (Similar plots for $\mathbf{X_c}$ formation are shown in supplemental figure S-2.)

$$\underset{\textbf{1}}{\text{Ru(P)(CO)}} + 2\text{NO} \overset{K_{NO}}{\rightleftharpoons} \underset{\mathbf{X}}{\text{Ru(P)(NO)}_2} + \text{CO} \qquad (8)$$

Two analogous dinitrosyl complexes, Ru(MPIXDME)$(NO)_2$ (MPIXDME = *meso*-porphyrin-IX-dimethyl ester) and Os(OEP)$(NO)_2$, have been claimed in the literature[12] but without structural characterization. The former was the product of reacting Ru(MPIXDME)(CO) with excess NO in benzene. This displayed a single ν_{NO} band at 1853 cm^{-1} in CH_2Cl_2 solution and optical and infrared spectra nearly identical to those of the structurally characterized complex Ru(OEP)(NO)(ONO).[12a] The latter was also prepared by reaction of Os(OEP)CO with excess NO in benzene and displayed a ν_{NO} band at 1778 cm^{-1} plus a lower frequency band at 1500 cm^{-1} consistent with a coordinated nitrite.[12b] Notably, reaction of Os(OEP)(CO) with NO in the presence of methanol gives the Os(OEP)(NO)(OMe) (i.e., formally NO^+) complex just as does the Ru analogue.[5] In this context, we conclude that it is very likely that the osmium "dinitrosyl" is also a nitrosyl-nitrite complex, i.e., Os(OEP)(NO)(ONO).

Mechanism for Formation of X? Under conditions of a large excess of NO where **X** formation is effectively irreversible, the rate of the first step is first order in [NO]. Furthermore, this step is suppressed by added CO or other donor ligands in the solution capable of occupying the sixth coordination site of Ru(P)(CO) (eq 2). In these contexts, Scheme 1 is proposed as a

(12) (a) Sruvastava, T. S.; Hoffman, L.; Tsutsui, M. *J. Am. Chem. Soc.* **1972**, *94*, 1385−1386. (b) Buchler, J. W.; Smith, P. D. *Chem. Ber.* **1976**, *109*, 1465−1476.

Scheme 1

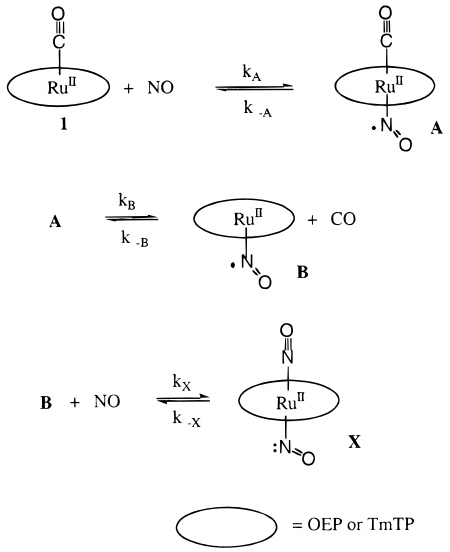

likely scenario for the formation of **X** from **1** in which the rate-limiting step is the dissociation of CO from the odd electron complex Ru(P)(CO)(NO) (**A**) with the rate constant k_b. **A** is likely to have its unpaired electron largely localized on the NO; however, any transfer of this to the Ru would involve the σ^* d_{z^2} orbital.[13] This would serve to labilize CO to give the uncharged, paramagnetic complex Ru(P)(NO) (**B**), which would react rapidly with NO to give the intermediate dinitrosyl complex **X**. However, it should be noted that in none of the various spectra recorded during the course of the reactions of **1** with NO were there any obvious indications of the less stable intermediates **A** and **B**. Hence, for Scheme 1 to be valid, each of these must be formed in low steady-state concentrations under the conditions of the experiments (see below).

If CO dissociation from **A** is rate limiting, the rate law of the first step would have the following form:

$$\frac{d[\mathbf{X}]}{dt} = k_B[\mathbf{A}] = k_B K_A[NO][\mathbf{1}] \quad (9)$$

where K_A ($= k_A/k_{-A}$) is the equilibrium constant for the formation of **A** from **1**. This treatment requires (i) K_A[NO] be $\ll 1$, (ii) that equilibrium between **1** and **A** is rapidly established on the time scale of the experiment, i.e., $k_{-A} \gg k_B$, and (iii) that k_X[NO] $\gg k_{-B}$[CO]. Under the conditions of the kinetics experiments illustrated by Figure 2 (large stoichiometric excess of NO, very low [CO]), the third of these criteria is easily met owing to the very low concentration of CO. Furthermore, k_X has been determined in flash photolysis experiments[14] to be 1×10^8 M^{-1} s^{-1} for Ru(OEP)(NO) and 5×10^7 M^{-1} s^{-1} for Ru(TmTP)(NO) (generated by NO_2 photolabilization from **2**). Thus, at millimolar concentrations of NO, the formation of **X** from **B** would be expected to be orders of magnitude faster than the absorbance changes seen in the first segment of the reactions observed by stopped flow techniques. The other two requirements are harder to establish quantitatively, although the absence of spectral changes consistent with formation of **A** is consistent with a small value for K_A. Furthermore, we have established (see above)[10] that substitution reactions involving adding various ligands to the sixth coordination site of **1** are quite rapid with second-order rate constants $k_L > 10^5$ M^{-1} s^{-1} and can assume that k_A will be similarly large. If so, the requirement that K_A[NO] be $\ll 1$ with millimolar NO provides a conservative lower limit for k_{-A} ($>10^3$ s^{-1}), which is sufficient to meet the second of the three criteria.

The suppression of the rate of the first step in the presence of other ligands can be easily explained in terms of a mechanism where the formation of **X** occurs by reaction of NO with Ru(P)(CO) exclusively. In such a case, formation of the ligand adduct Ru(P)(CO)L (eq 2) is a "dead-end" equilibrium, and the following relationship would result.

$$k_{obs}(1)' = \frac{k_{obs}(1)}{(1 + K_L[L])} \quad (10)$$

where $k_{obs}(1)'$ is the pseudo first-order rate constant in the presence of the ligand L and $k_{obs}(1)$ is that rate constant in dry toluene without added L.

Mechanism for Formation of 2? The second, slower stage in the overall process indicated by eq 1 is the conversion of **X** to **2**, accompanied by reduction of NO to N_2O, i.e.,

$$\underset{\mathbf{X}}{Ru(P)(NO)_2} + 2NO \overset{k_{obs}(2)}{\rightleftharpoons} \underset{\mathbf{2}}{Ru(P)(NO)(ONO)} + N_2O \quad (11)$$

The apparent rate law for this transformation is second order in [NO] and first order in the concentration of the ruthenium substrate **X**, i.e.,

$$\frac{d[\mathbf{2}]}{dt} = k_2[NO]^2[\mathbf{X}] \quad (12)$$

Notably, this rate law is inconsistent with one mechanism we considered (prior to these kinetics studies) to account for N_2O production, namely, a disproportionation pathway involving two ruthenium centers in the rate-limiting step.[5a] If that were the case, the rate should have been dependent on the concentration of **X** *squared*, so this pathway is ruled out.

Two alternative mechanisms involving but a single metal center are illustrated in Schemes 2 and 3. These have in common a preequilibrium involving NO, followed by an irreversible atom transfer step. In both cases, the kinetics are consistent with eq 12, if the atom transfer step is rate limiting.

First, let us consider the plausibility of Scheme 2, which is inherently attractive owing to its simplicity. NO is well-known to form dimers, and the structure of the tail to tail dimer with the two nitrogens linked has been characterized both in the gas phase[15] and in the solid state.[16] So it is reasonable to expect formation of similar dimers in solution. NO dimerization in the gas phase has been reported to have a ΔH_f of -2.3 kcal mol^{-1},[17] and an equilibrium constant K_d of $< 3 \times 10^{-4}$ M^{-1} at 306 K has been estimated from spectroscopic data in the gas phase.[18] According to Scheme 2, the rate of the reaction would be $k_{ox}K_d$[NO]^2[**X**], and $k_2 = k_{ox}K_d$. If one assumes the same value for K_d in toluene solution as in the gas phase, this requires a value

(13) Enemark, J. H.; Feltham, R. D. *J. Am. Chem. Soc.* **1974**, *96*, 5002−5004.

(14) (a) Lorkovic, I. Miranda, K. M.; Lee, B.; Bernhard, S.; Schoonover, J.; Ford, P. C. *J. Am. Chem. Soc.* **1998**, *120*, 11674−11683. (b) The intermediate Ru(P)(NO) is generated by the labilization of NO_2 as one photoreaction pathway of Ru(P)(NO)(ONO), and the rates of NO trapping of this reactive intermediate were determined by time-resolved optical spectroscopy.

(15) Kukolich, S. G. *J. Am. Chem. Soc.* **1982**, *104*, 4715−4716.

(16) Lipscomb, W. N.; Wang, F. E.; May, W. R.; Lippert, E. L. *Acta Crystallogr.* **1961**, *14*, 1100−1101.

(17) Fischer, I.; Strobel, A.; Staecker, J.; Niedner-Schatteburg, G.; Muller-Dethlefs, K.; Bondybey, V. E. *J. Chem. Phys.* **1992**, *96*, 7171−7174.

(18) Forte, E.; van den Bergh, H. *Chem. Phys.* **1978**, *30*, 325−331.

Scheme 2

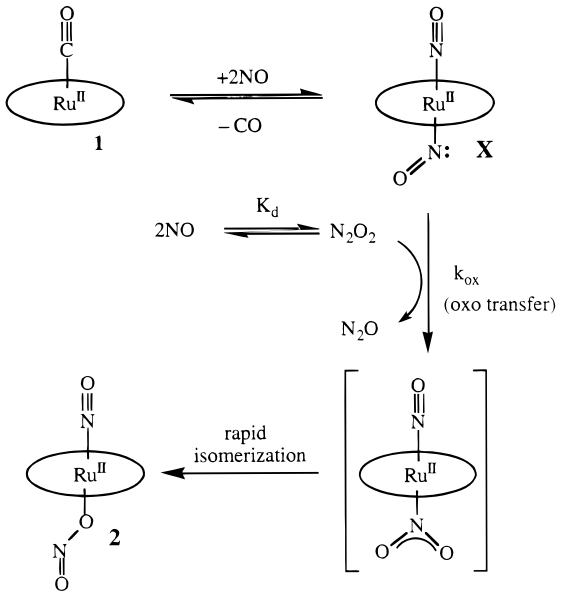

$$\frac{d[\mathbf{2}]}{dt} = k_{ox}K_d[NO]^2[\mathbf{X}]$$

Scheme 3

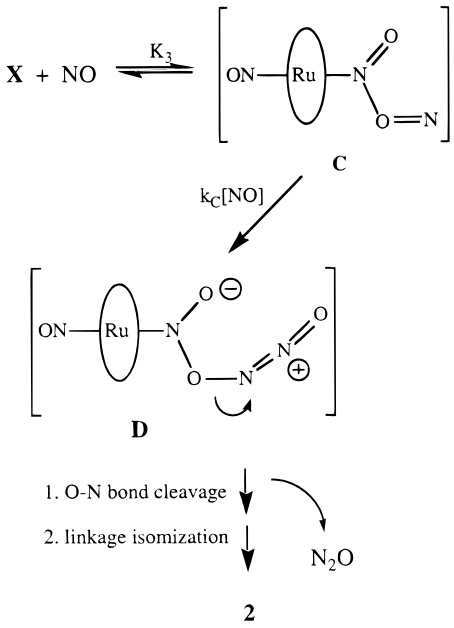

$$\frac{d[\mathbf{2}]}{dt} = k_C K_3[NO]^2[\mathbf{X}]$$

for k_{ox} equal to k_2/K_d, i.e., $> 6 \times 10^8$ M^{-1} s^{-1}. Considerable uncertainty here lies in the magnitude of the estimated K_d; however, if this value is anywhere near correct, the resulting estimate of k_{ox} is much too large for an atom transfer reaction coupled to considerable electronic and nuclear reorganization. Such consideration appears to argue against the viability of Scheme 2.

Scheme 3 is similar to mechanisms previously proposed to account for disproportionation of NO by metal complexes.[8b,c] In such mechanisms, the metal center serves as a template for the assembly of NO oligomers of various fanciful structures that then can reorganize, sometimes with redox participation of the metal, to the disproportionation products N_2O and NO_2 (or NO_2^-). If formation of a species such as **D** were rate limiting, the rate law for the formation of **2** (eq 14) would be consistent with the third-order kinetics described by eq 12; i.e., $k_2 = k_C K_3$. However, we have no spectroscopic evidence in this study for the formation of species **C** or **D**. Furthermore, for other systems where similar NO disproportionation facilitated by transition metal complexes has been described and species similar to **C** or **D** have been proposed,[8b,c] spectroscopic evidence supporting the formation of such intermediates is notably lacking. While these types of structures are not implausible, acceptance of this speculative mechanism awaits more concrete evidence.

Summary

The kinetics and time-resolved spectroscopic results described above indicate that the reaction of Ru(P)(CO) with NO proceeds in two key stages. The first stage is the reversible reaction to form the dinitrosyl complex $Ru(P)(NO)_2$. Under conditions of a large excess of NO where this addition/substitution reaction is effectively irreversible, the rate of the forward reaction to form **X** displays an apparent rate law which is first order in [NO] and is suppressed by added CO or other ligands which may coordinate the sixth coordination site of Ru(P)(CO). It is concluded that, under excess NO, the rate-limiting step of this first stage is the dissociation of CO from an intermediate species of the composition Ru(P)(NO)(CO).

The second, slower stage is the conversion of the dinitrosyl complex to the nitrosyl nitrito analogue accompanied by reduction of NO to N_2O via a rate law second order in [NO].

$$Ru(P)(NO)_2 + 2NO \xrightarrow{k_{obs}(2)} Ru(P)(NO)(ONO) + N_2O \quad (13)$$

Two schemes are proposed as possible mechanisms, one involving a simple oxygen atom transfer from the transitory nitric oxide dimer ONNO to coordinated NO (Scheme 2), the other utilizing the Ru center as a template to assemble an oligomer of NO which decomposes to nitrous oxide plus coordinated NO_2 (Scheme 3). However, gas-phase studies suggest that the NO dimerization constant K_d is quite small. If so, Scheme 2 would require an unreasonably large value for the rate constant k_{ox} (oxygen transfer from ONNO) to satisfy the rate of the second. Thus it appears that assembly of several NO equivalents on a single metal center prior to N_2O formation, e.g. Scheme 3, is a more likely pathway for eq 13.

Acknowledgment. This work was supported by the National Science Foundation (CHE-9400919 and CHE-9726889). The stopped flow spectrophotometer was purchased with an instrumentation grant from the National Science Foundation (CHE 9522259). Groundwork studies on the syntheses of Ru(P)(NO)(ONO) complexes as well as preliminary studies indicating intermediates in the reaction of Ru(P)CO with NO were carried out by Dr. Katrina M. Miranda, and these studies are described in her Ph.D. Dissertation (ref 5b).

Supporting Information Available: Supplemental figures: Figure S-1: Custom-designed tonometer for use with air-sensitive solutions on a stopped flow spectrophotometer. Figure S-2: Plots of ΔA^{-1} vs $[NO]^{-1}$ and vs $[NO]^{-2}$ analogous to Figure 5 to determine the number of NO molecules involved in forming the TmTP complex $\mathbf{X_c}$ from **1c**. This material is available free of charge via the Internet at http://pubs.acs.org.

IC981121R